

Addressing overlapping communities in multiple-source detection: An edge clustering approach for complex networks

Haomin Li¹, Daniel K. Sewell^{1*}

¹ Department of Biostatistics, University of Iowa, Iowa City, IA, USA

* daniel-sewell@uiowa.edu

Abstract

The source detection problem in network analysis involves identifying the origins of diffusion processes, such as disease outbreaks or misinformation propagation. Traditional methods often focus on single sources, whereas real-world scenarios frequently involve multiple sources, complicating detection efforts. This study addresses the multiple-source detection (MSD) problem by integrating edge clustering algorithms into the community-based label propagation framework, effectively handling mixed-membership issues where nodes belong to multiple communities.

The proposed approach applies the automated latent space edge clustering model to a network, partitioning infected networks into edge-based clusters to identify multiple sources. Simulation studies on ADD HEALTH social network datasets demonstrate that this method achieves superior accuracy, as measured by the F1-Measure, compared to state-of-the-art clustering algorithms. The results highlight the robustness of edge clustering in accurately detecting sources, particularly in networks with complex and overlapping source regions. This work advances the applicability of clustering-based methods to MSD problems, offering improved accuracy and adaptability for real-world network analyses.

Introduction

The source detection problem is a critical topic in network analysis. It involves identifying the origin or source(s) responsible for diffusion processes, such as the outbreak of epidemics, the spread of gossip over online social networks, the propagation of computer viruses over the Internet, and the adoption of innovations [1]. Identifying these sources is crucial because it allows for targeted interventions, which are often more effective and efficient than broader, less focused strategies, and leads to a better understanding of the diffusion process.

In epidemiology, for example, determining the initial carrier of a disease (often referred to as "patient zero") can inform precise containment strategies that prevent further transmission and save lives. Similarly, in cybersecurity, identifying the origin of a malware attack or computer virus enables rapid neutralization, minimizing damage and protecting vulnerable systems [2].

Beyond healthcare and cybersecurity, source detection is essential in managing the spread of misinformation in social networks. Identifying the originator of false information allows platforms to intervene early, reducing the harmful impact on public opinion and social behavior. In marketing, understanding the key influencers or early adopters who drive the spread of new products or ideas can help optimize promotional strategies and accelerate diffusion [3].

The effectiveness of source detection methods depends on the type of network observations utilized. In this study, we focused on snapshot-based observations. A snapshot provides a view of the network at a specific point in time, offering information about the nodes that are infected at the time of observation and the probability of infection for those nodes that have already been exposed to the diffusion process [4].

Most source detection research assumes that there is a single source in the network when studying the diffusion process [5]. However, in reality, the spread of misinformation or infections often originates from multiple sources rather than a single point. For example, during the early stages of the COVID-19 pandemic, the virus spread from multiple locations, as international and domestic travel facilitated the simultaneous introduction of the virus into a given locale. Similarly, diseases like Ebola and Zika often have multiple sources of outbreaks, especially when the disease is transmitted from animals to humans in different regions. These multiple introductions complicate the containment process and require detection methods that can identify more than one source of infection within a network of disease transmission [6, 7].

Few researchers have focused on multiple sources detection (MSD) problem. One such method builds off of the Rumor Centrality, initially designed for single-source detection, in order to handle multiple sources by considering infection times and network topology, thereby allowing for identification of multiple origins in the diffusion process [3]. Another method, Backtracking Source Identification, works by reversing the infection spread, attempting to retrace the diffusion paths to pinpoint the potential origins of the spread [8].

Zang et.al [9] first proposed a clustering-based method for the MSD problem. Their method involves first performing clustering on the infected network to partition it into distinct groups. Once the clustering structure is identified, a single-source detection algorithm is applied within each cluster to locate the sources independently [10].

Simulation studies have shown that treating MSD as a series of single-source detection problems is insufficient. This limitation may arise in part from disregarding the influence and interactions between neighboring clusters. To overcome this, Zhang et.al [11] introduced a community-based label propagation (CLP) framework, building on the work of Wang et.al [12]. The CLP framework begins with clustering the infection network but improves detection accuracy by incorporating node prominence and exoneration effects, where nodes surrounded by more infected nodes and fewer non-infected nodes are more likely to be identified as sources.

A significant limitation of current clustering-based MSD algorithms is their failure to account for the mixed-membership issue caused by the diffusion process. (Mixed-membership refers to the ubiquitous situation in which nodes belong to more than one cluster.) Fig 1 illustrates the application of a clustering algorithm for the MSD problem. In the left plot, red nodes represent the sources of infection. The middle plot shows the infection pattern after a certain period, where the enlarged nodes denote infected individuals. Typically, the infection originates from the sources and spreads locally, affecting nearby nodes and forming distinct clusters or communities centered around each source. However, as shown in the right plot, black nodes represent infected individuals influenced by more than one source. This demonstrates the mixed-membership problem, where nodes belong to multiple communities. Ignoring this issue can lead to overestimating the number of clusters in the detection process.

Edge clustering algorithms offer a powerful solution to this challenge by clustering edges rather than nodes, thereby capturing relationships between nodes and accounting for scenarios where nodes belong to multiple sources or communities. Key algorithms in this domain include the Latent Space Edge Clustering (LSEC) model [13], which clusters edges based on latent features of nodes; and the automated Latent Space Edge Clustering (aLSEC) model [14], which builds on LSEC by automating the determination

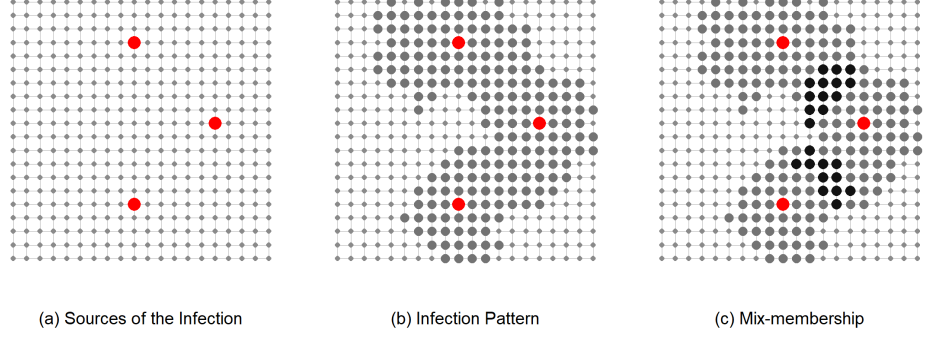


Fig 1. Visualization of a MSD problem on a grid graph. The left panel identifies the sources of infection (red nodes), while the middle panel shows the resulting infection pattern, with enlarged nodes representing infected individuals forming clusters around each source. The right panel demonstrates the mixed-membership issue, where black nodes are influenced by multiple sources.

of the number of clusters, which incorporates edge weights and accounts for noisy or anomalous edges. These models represent significant advancements in edge clustering by addressing limitations in traditional node-based methods, particularly in handling mixed-membership.

Building on these developments, this paper integrates the edge clustering framework with existing multiple-source detection solutions, specifically the Community-based Label Propagation (CLP) framework. By leveraging the ability of edge clustering to address mixed-membership, the proposed approach enhances the precision and accuracy of source detection.

In Section Algorithm, we detail the entire process of our proposed algorithm. Section Simulation Design presents the results of a simulation study designed to evaluate the effectiveness of this method. In Section Result, we summarize the outcomes of the simulations, while Section Discussion provides a discussion of the key findings and their implications.

Algorithm

Our proposed algorithm builds upon the CLP framework, extending it to account for the possibility that nodes may belong to multiple sources. We begin with the full network, denoted as $G = (\mathcal{V}, \mathcal{E})$, where \mathcal{V} is the set of nodes and $\mathcal{E} \subset \mathcal{V} \times \mathcal{V}$ is the set of edges between elements of \mathcal{V} . Given the full network G , the observed infected sub-network is represented as $G_I := (\mathcal{V}_I, \mathcal{E}_I)$, where $\mathcal{V}_I \subseteq \mathcal{V}$ and $\mathcal{E}_I = \mathcal{E} \cap (\mathcal{V}_I \times \mathcal{V}_I)$. In this scenario, it is assumed that all infected or influenced nodes are fully observed. We additionally consider information about uninfected boundary nodes, denoted as \mathcal{V}_{UB} , which are adjacent to at least one infected neighbor. Together, the infected sub-network and the boundary nodes form the extended infected network, $G_{EI} = (\mathcal{V}_{EI}, \mathcal{E}_{EI})$, where $\mathcal{V}_{EI} = \mathcal{V}_{UB} \cup \mathcal{V}_I$ and $\mathcal{E}_{EI} = \mathcal{E} \cap (\mathcal{V}_{EI} \times \mathcal{V}_{EI})$. The objective of the algorithm is to identify the original infection source set, $S \subset \mathcal{V}_I$.

Edge Clustering

Let G_I consist of N_I nodes and M_I edges. The edge set $\mathcal{E}_I = \{e_m\}_{m=1}^{M_I}$ represents the edges in G_I , where each edge is defined as $e_m = (e_{m1}, e_{m2})$, with e_{m1} being the sending

node and e_{m2} the receiving node. We apply an edge clustering algorithm on G_I , detecting K distinct clusters. Rather than prespecifying K , by using the aLSEC algorithm K is automatically determined in a data-driven manner. See [14] for more details. Let $Z_{mk} \in \{0, 1\}$ indicate whether edge e_m belongs to cluster k .

Label Assignment

For any infected node u , the node's age is defined as in [15]:

$$A_u^I = \frac{I_u}{O_u}(1 + \log O_u)$$

where I_u represents the number of infected neighbors of node u (i.e., the degree of node u in the infection network G_I) and O_u is node u 's degree in the original network G . For any uninfected node v in G_{EI} , the age is defined as:

$$A_v^U = \frac{\sum_{u \in N_I(v)} I_u}{I_v}$$

where $N_I(v)$ denotes the set of infected neighbors of node v , and as before $I_u = |N_I(u)|$ is the number of infected neighbors.

The concept of node age for both infected and uninfected nodes is introduced to evaluate their prominence and incorporate exoneration effects. The prominence effect suggests that nodes surrounded by a larger proportion of infected neighbors are more likely to be identified as the infection sources, as their prominence in the network makes them strong candidates for initiating the spread. Conversely, the exoneration effect posits that neighboring nodes can act like alibis, reducing the likelihood of a node being the source. For example, if a node is infected but surrounded by a high proportion of uninfected neighbors, this lowers the probability of that node being the true source, as the uninfected neighbors provide evidence against the node being responsible for the spread [15].

Following the edge clustering in the first step, K clusters are obtained for the infected network G_I . We then consider the extended infected network G_{EI} , which includes N_{EI} nodes ($N_{EI} \geq N_I$). We construct a $N_{EI} \times (K + 1)$ label matrix \mathcal{L}^t , where t represents the iteration number. Initially, we set \mathcal{L}^0 using the results from the edge clustering in the following way. For $k = 1, \dots, K$, set

$$\begin{aligned} \mathcal{L}_{ik}^0 &:= \begin{cases} A_i^I & \text{if } i \in \mathcal{V}_I \text{ and } \exists m : Z_{mk} = 1 \ \& \ e_{m1} = i \cup e_{m2} = i \\ 0 & \text{otherwise,} \end{cases} \\ \text{and } \mathcal{L}_{i(K+1)}^0 &:= \begin{cases} \max_{v \in \mathcal{V}_{UB}} (A_U(v)) - A_U(i) & \text{if } i \in \mathcal{V}_{UB} \\ 0 & \text{otherwise} \end{cases} \end{aligned} \quad (1)$$

The reasoning behind this assignment is that older uninfected nodes exert a weaker exoneration effect on their infected neighbors, as their prominence reduces with increasing age.

Label Propagation

The label matrix \mathcal{L} is propagated iteratively throughout the network. In each iteration, nodes in the extended infected network update their labels by incorporating both the prominence and exoneration effects from their neighboring nodes. Nodes with higher prominence are more likely to propagate stronger labels (ages) to their neighbors.

$$\mathcal{L}^{t+1} = \alpha \mathcal{A} \mathcal{L}^t + (1 - \alpha) \mathcal{L}^0$$

where \mathcal{A} represents the symmetrically normalized adjacency matrix of the extended infection graph G_{EI} , and $0 < \alpha < 1$ is the weight that determines the proportion of label information each node receives from its neighbors versus its initial value. In this study we set α to be 0.5.

It has been proven that the label matrix \mathcal{L}^t will converge to a stationary value: [12]

$$\mathcal{L}^* = (1 - \alpha)(I - \alpha \mathcal{A})^{-1} \mathcal{L}^0$$

Source Identification

After obtaining the converged label matrix \mathcal{L}^* , we then row-normalize \mathcal{L}^* to obtain node-specific cluster source scores. The node in \mathcal{V}_I with the highest score in each of the first K columns of the row-normalized \mathcal{L}^* is selected as the infection source for the corresponding community. Mathematically, the source node for community k , denoted as S_k , is given by:

$$S_k = \arg \max_{i \in \mathcal{V}_I} \mathcal{L}^*[i, k] \quad \text{for } k = 1, 2, \dots, K$$

Simulation Design

The simulation study was built on the real-world datasets. We selected three networks from Adolescent Health, or ADD HEALTH Networks [16] in the networkdata R package [17]. The ADD HEALTH data is based on a 1994-95 survey where 90,118 students from 84 communities participated, representing school-based social networks. In some communities, there were two schools, allowing students to name friends from a “sister school.” Each student filled out a questionnaire, naming up to five male and five female friends.

We selected three networks from the ADD HEALTH dataset: addhealth15, addhealth20, and addhealth75. Table 1 summarizes the features of these networks. At the start of each simulation, K sources were randomly selected from each network, and the infection process was simulated with an infection probability of 0.2. The spread continued until over 10% of the nodes in the network were infected. Different clustering algorithms were then applied within the CLP framework. Specifically, we tested three methods: (1) Louvain, (2) Leading Eigenvector, and (3) aLSEC. Louvain clustering and the Leading Eigenvector method are widely recognized as state-of-the-art node clustering algorithms for addressing clustering-based source detection problems [10, 11].

Table 1. The Description of Datasets.

Network	# Nodes	# Edges	Ave. degree	Density
addhealth15	1089	5370	9.86	0.0045
addhealth20	922	5229	11.34	0.0062
addhealth75	1011	5459	10.80	0.0053

For each network, we set the number of sources K to 1, 3, and 5. Under each configuration, we conducted 200 simulations with varying random seeds. The accuracy of each source detection approach was evaluated using the F1-Measure [18], which combines precision and recall to provide an overall performance metric.

Computation for the simulation study was done on University of Iowa High-performance Computing (HPC) system. The tests of model computation time

were performed on a server with an Intel(R) Xeon(R) Gold 6230 CPU @ 2.10 GHz. All code was executed by R in version 4.0.5 [19].

Result

The simulation results presented in Figure 2 demonstrate that the aLSEC model consistently outperforms both the Louvain and Leading Eigenvector clustering algorithms across all three selected ADD HEALTH networks (addhealth15, addhealth20, and addhealth75). The y-axis represents the F1-Measure, which evaluates the accuracy of source detection, while the x-axis shows the number of sources tested ($K = 1$, $K = 3$, and $K = 5$).

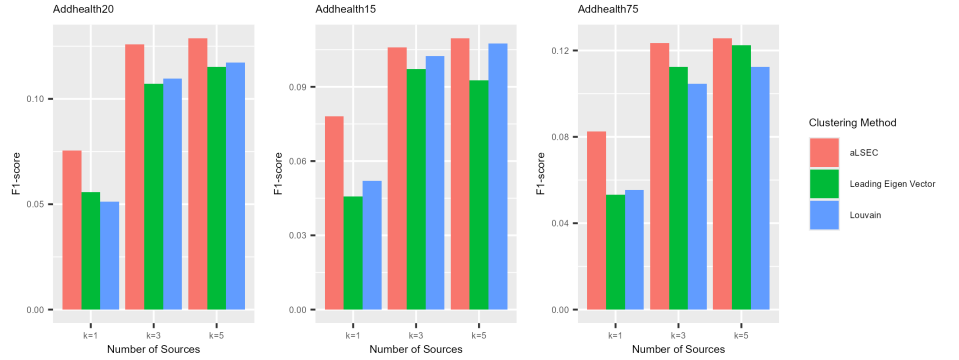


Fig 2. Simulation Results. Comparison of F1-Measure performance across clustering methods for multiple-source detection (MSD) in three ADD HEALTH networks: Addhealth20, Addhealth15, and Addhealth75. Each panel corresponds to a different network.

In all cases, the aLSEC model achieves the highest F1-Measure scores, indicating its superior performance in accurately detecting the true sources of infection or diffusion in these networks. This trend holds across both single-source and multiple-source detection scenarios, with the difference in performance being particularly pronounced when $K = 1$. This suggests that the aLSEC model is especially effective in smaller-scale infection detection settings, where it avoids the common pitfall of overestimating the number of clusters, a limitation that both the Louvain and Leading Eigenvector methods encounter due to their failure to account for the mixed-membership issue.

Discussion

This work utilizes edge clustering algorithms to address the multiple source detection (MSD) problem, focusing on the challenges of overlapping communities and mixed-membership in diffusion processes. By incorporating edge clustering into the CLP framework, we enhance traditional community-based detection methods to effectively handle scenarios where nodes are influenced by multiple sources. Simulation results demonstrate the superiority of this approach, particularly in achieving greater accuracy in multiple-source detection compared to conventional methods such as Louvain and Leading Eigenvector.

However, certain limitations remain. Firstly, this study focused on unweighted networks, utilizing the aLSEC model for edge clustering. While effective, many real-world networks involve weighted edges, where connection strengths vary across

relationships. A promising extension would be incorporating the WECAN model [20], an edge clustering algorithm designed for weighted networks, which builds on aLSEC by directly accounting for edge weights. Incorporating edge weights could enhance source detection accuracy by distinguishing between stronger and weaker connections.

Additionally, this study relies on a "snapshot" observation of the network, capturing the state of infection at a single point in time. This static approach may limit the ability to fully capture the dynamics of diffusion processes. Extending the methodology to dynamic networks, where the temporal evolution of the spread is accounted for, could lead to more accurate and timely identification of sources by incorporating changes in the network structure and infection status over time. Addressing these limitations will enhance the robustness and applicability of the edge clustering algorithm for multiple-source detection, further solidifying its potential as a versatile tool for diverse network-based applications.

Acknowledgments

This work was supported by the US Centers for Disease Control and Prevention (5 U01CK000594-04-00) as part of the MInD-Healthcare Program (<https://www.cdc.gov/healthcare-associated-infections/php/research/mind-healthcare.html>).

Data availability

Data used in our simulation study are publicly available through the R package `networkdata` [17].

References

1. Zhu K, Ying L. Information source detection in the SIR model: A sample-path-based approach. *IEEE/ACM Transactions on Networking*. 2014;24(1):408–421.
2. Antulov-Fantulin N, Lančić A, Šmuc T, Štefančić H, Šikić M. Identification of patient zero in static and temporal networks: Robustness and limitations. *Physical review letters*. 2015;114(24):248701.
3. Shah D, Zaman T. Detecting sources of computer viruses in networks: theory and experiment. In: *Proceedings of the ACM SIGMETRICS international conference on Measurement and modeling of computer systems*. ACM; 2010. p. 203–214.
4. Zhu K, Ying L. A robust information source estimator with sparse observations. *Computational Social Networks*. 2014;1:1–21.
5. Shelke S, Attar V. Source detection of rumor in social network—a review. *Online Social Networks and Media*. 2019;9:30–42.
6. Holmdahl I, Buckee C. Wrong but useful—what COVID-19 epidemiologic models can and cannot tell us. *New England Journal of Medicine*. 2020;383(4):303–305.
7. Waldman L, Marani M, Martínez G, Steinacher M, Mangili A, Holmes EC, et al. Epidemiology of Ebola virus disease in the Democratic Republic of the Congo, 1976-2014. *Emerging Infectious Diseases*. 2020;26(2):282.

8. Dong W, Zhang W, Tan CW. Rooting out the rumor culprit from suspects. In: 2013 IEEE international symposium on information theory. IEEE; 2013. p. 2671–2675.
9. Zang W, Zhang P, Zhou C, Guo L. Discovering multiple diffusion source nodes in social networks. *Procedia Computer Science*. 2014;29:443–452.
10. Zang W, Zhang P, Zhou C, Guo L. Locating multiple sources in social networks under the SIR model: A divide-and-conquer approach. *Journal of Computational Science*. 2015;10:278–287.
11. Zhang C, Fu L, Long F, Wang X, Zhou C. CLP: A Community based Label Propagation Framework for Multiple Source Detection. In: IEEE INFOCOM 2023-IEEE Conference on Computer Communications. IEEE; 2023. p. 1–10.
12. Wang Z, Wang C, Pei J, Ye X. Multiple source detection without knowing the underlying propagation model. In: *Proceedings of the AAAI Conference on Artificial Intelligence*. vol. 31; 2017.
13. Sewell DK. Model-based edge clustering. *Journal of Computational and Graphical Statistics*. 2021;30(2):390–405.
14. Pham HT, Sewell DK. Automated detection of edge clusters via an overfitted mixture prior. *Network Science*. 2024; p. 1–19.
15. Ali SS, Anwar T, Rastogi A, Rizvi SAM. EPA: Exoneration and prominence based age for infection source identification. In: *Proceedings of the 28th ACM International Conference on Information and Knowledge Management*; 2019. p. 891–900.
16. Moody J. Peer influence groups: identifying dense clusters in large networks. *Social networks*. 2001;23(4):261–283.
17. Almquist ZW. networkdata: Lin Freeman’s Network Data Collection; 2014. Available from: <https://github.com/zalmquist/networkdata>.
18. Van Rijsbergen CJ. *Information retrieval*. 2nd. newton, ma; 1979.
19. R Core Team. *R: A Language and Environment for Statistical Computing*; 2023. Available from: <https://www.R-project.org/>.
20. Li H, Sewell DK. Model-based edge clustering for weighted networks with a noise component. *Computational statistics & data analysis*. 2025;209:108172.